**Title**

DISLOCATION MECHANISMS OF MOLYBDENUM SINGLE CRYSTALS AT LOW TEMPERATURES

**Permalink**

**Author**

Lau, Silvanus Siu-Wai.

**Publication Date**

1966

# University of California

# Ernest O. Lawrence Radiation Laboratory

DISLOCATION MECHANISMS OF MOLYBDENUM SINGLE CRYSTALS
AT LOW TEMPERATURES

# DISCLAIMER

UNIVERSITY OF CALIFORNIA

Lawrence Radiation Laboratory
Berkeley, California

AEC Contract No. W-7405-eng-48

# DISLOCATION MECHANISMS OF MOLYBDENUM SINGLE CRYSTALS
## AT LOW TEMPERATURES

Silvanus Siu-Wai Lau

(M.S. Thesis)

January, 1966

DISLOCATION MECHANISMS OF MOLYBDENUM SINGEL CRYSTALS
AT LOW TEMPERATURES

Silvanus Siu-Wai Lau

Inorganic Materials Research Division, Lawrence Radiation Laboratory,
and Department of Mineral Technology, College of Engineering,
University of California, Berkeley, California

January, 1966

## ABSTRACT

The effects of temperature and strain rate on flow stress of molybdenum single crystals were investigated. The flow stress increased slightly as the temperature decreased from approximately 600°K to 425°K. A rapid increase in flow stress then occurred upon testing at lower temperatures. The strong temperature and strain rate dependence of the flow stress (below 425°K) were rationalized satisfactorily in terms of the Dorn and Rajnak theory of the Peierls' mechanism of plastic deformation. Above 425°K, the experimental results did not agree exactly with the theory, which indicates that there might be some other, as yet unidentified, thermally activated mechanism operative in this region.

# INTRODUCTION

Recently, considerable interest has been focused upon the low

temperature plastic behavior of b.c.c. refractory metals, mainly Mo,

Ta, Nb and W. The flow stress of these metals depends strongly on temperature

and strain rate over the low temperature region (T < 0.2 $T_{melting}$). A

basic understanding of their mechanical behavior necessitates a thorough

investigation of the rate-controlling mechanism of the mobile dislocations.

A few thermally-activated dislocation mechanisms have been proposed, in

chronological order; these are:

    (1) Breaking away from an interstitial atmosphere,

    (2) Overcoming the Peierls'-Nabarro stress,

    (3) Nonconservative motion of jogs,

    (4) Overcoming interstitial precipitates,

    (5) Cross-slip.

It was concluded by Conrad,[1] Dorn and Rajnak,[2] and Christian and Masters[3]

that the overcoming of the Peierls'-Nabarro stress which arises from the

covalent bondings between atoms in b.c.c. metals was the most satisfactorily

explained rate controlling mechanism.

Several models of the Peierls' mechanism have been formulated.[2,4-6]

Experimental results obtained from the deformation of Fe, V, Nb, Ta,[3]

AgMg,[7] $Ag_2Al$,[8] Fe-2% Mn alloy[9] have been sucessfully explained by the

Dorn-Rajnak model of nucleation of kink pairs.

The purpose of this work was to investigate the mechanical behavior

of zone refined single crystals of molybdenum at low temperatures

and to correlate experimental results with the Peierls' mechanism using

the Dorn and Rajnak model.

Molybdenum has the attractive properties of high melting point (2883°K), a relatively low density (10.22 g/cc), a high modulus of elasticity (46 x 10$^6$ psi) and excellent strength to density ratio at high temperature.[10] Fundamental knowledge of the mechanical behavior can best be obtained by the investigation of high purity single crystals. Crystals of this type can be grown with an Electron Beam Floating Zone apparatus.

It is well known that interstitial impurity level and dislocation density have a strong influence on the flow stress. Specimens were, therefore, given the same number of refining passes in order to achieve approximately the same high purity level. Each was prestrained to the same stress level at the same temperature in the athermal region where thermal fluctuation had no effect on the flow stress in order to achieve approximately equal dislocation density in each specimen.

It will be shown that the strong dependence of temperature and strain rate can be satisfactorily explained by the rate of nucleation of pairs of kinks on dislocations involved in the Peierls' mechanism for plastic deformation.

### DORN AND RAJNAK'S MODEL OF PEIERLS' MECHANISM[2]

When a straight-dislocation line lies in a potential valley parallel to lines of closest packing of atoms on the slip plane, it has its lowest energy. When such a straight dislocation line moves from one valley to the next, the core energy of the dislocation increases due to the change of position and bond angles. The core energy of the dislocation was assumed to reach a maximum midway between the two adjacent valleys. A small displacement will cause the dislocation to fall from the maximum position into the next valley which is a minimum energy position for the dislocation. The shear stress necessary to promote such motion of dislocation at the absolute zero is known as the Peierls' stress, $\tau_p$.

A forward motion of such kind can be achieved by the nucleation of a pair of kinks under the influence of an applied stress and a thermal fluctuation. When the size of this kink pair has reached a critical value, the two kink segments will move away from each other under the influence of the applied stress, resulting in a forward motion of the dislocation by a displacement, a, equal to the periodicity of the rows of closely spaced atoms on the slip plane.

Dorn and Rajnak applied the suggestion of Friedel that the major factor involved in kink nucleation is the additional energy due to the increased line length of the dislocation to formulate their model: The shape of the Peierls' hill was approximated by

$$\Gamma\{y\} = \frac{\Gamma c + \Gamma o}{2} + \frac{\Gamma c - \Gamma o}{2}\left(\frac{\alpha}{2} + \cos\frac{2\pi y}{a} - \frac{\alpha}{4}\cos\frac{4\pi y}{a}\right)$$

where $\Gamma o$ and $\Gamma c$ are the energies per unit length of a dislocation lying

at the top and bottom of the Peierls' hill, respectively, $\alpha$ is a hill-shape factor that was assumed to vary between -1 and 1.

The difference in energy of a displaced dislocation line (AB'C in Fig. 1) and that of the corresponding straight dislocation line lying along $y = y_o$ is given by

$$U_n = \int_{-\infty}^{\infty} \left( \Gamma\{y\} \sqrt{1 + \frac{dy}{dx}^2} - \Gamma\{y_o\} - \tau^* b (y - y_o) \right) dx$$

where the first two terms of the intergrand are the line energies of the dislocation in the two positions, and the third term gives the extra work done by the stress $\tau^*$ in displacing the dislocation from $y_o$ to $y$. Using Euler's condition for minimizing the energy, the critical energy for nucleating one pair of kinks was calculated. Upon numerical integration of the above equation, Dorn and Rajnak were able to obtain universal relationships between $U_n/2U_k$ and $\tau^*/\tau_p$ ($U_k$ is the kink energy), activation volume and applied stress, and between the velocity of the dislocation and the applied stress.

## EXPERIMENTAL PROCEDURE

Single crystal specimens of molybdenum were prepared and tested in the following manner.

(1) Molybdenum rods (1/4 in. in dia) of commercial purity were given two refining passes using an Electron Beam Floating Zone apparatus (MRC EBZ-93A model).

(2) The zone refined rods were then oriented with the same apparatus in such a manner that the $(\bar{1}01)$ [111] slip system was operative when tensile specimens were prepared. Slip in b.c.c. metals tends to occur in well-defined directions <111>, but on less well-defined planes.[12] It was important to orient the crystal such that the $(\bar{1}01)$ plane had the maximum resolved shear stress and an ample single slip region. Two seeding runs were made to insure that the desired orientation was achieved (Fig. 2).

(3) The initial orientation $\chi_0$ and $\lambda_0$ of each crystal was determined by the Laue back-reflection technique.

(4) Single crystals were made into specimens of approximately 1.75 in. in length, 0.8 in. in guage section and 0.1 in. in diameter.

(5) The machined guage section of each specimen was electropolished in a bath containing 175 ml $CH_3OH$ and 25 ml $H_2SO_4$ at $0°C$ to remove all deformation put into the specimen during machining.

(6) Resistivity measurements were made on the electropolished specimens at $273°K$, $77°K$ and $4.2°K$. The ratio of resistivities at $273°K$ and $4.2°K$ was used to estimate the purity.

(7) Each specimen was prestrained to the same stress level (3.11

x $10^8$ dynes/$cm^2$) at 550°K to minimize scatter from specimen to specimen.

(8) Tension tests at different temperatures were performed at strain rates of 9.2 x $10^{-3}$ sec$^{-1}$ and 9.9 x $10^{-5}$ sec$^{-1}$. For testing temperatures below 77°K, a cryostat apparatus was used. Stress was determined to within ±3 x $10^6$ dynes/$cm^2$ and tensile strains were measured to within ±0.001.

## EXPERIMENTAL RESULTS AND DISCUSSION

### Resistivity ratio and impurity level.

Resistivity measurements were made using a "four-lead" potential probe, an external resistor and a constant D.C. current supply.[14] The specific resistivity is given by

$$\rho = \frac{E}{I} \frac{A}{L}$$

where $\rho$ = specific resistivity of the crystal

$A$ = cross section area

$E$ = potential across the specimen

$I$ = current

$L$ = length between two contact points.

The resistivity ratios, $\frac{\rho 4.2^{\circ}K}{\rho 273^{\circ}K}$, of four zone passes molybdenum single crystals were all of the order of $10^3$. Chemical analysis by the vacuum fusion method of some of these crystals yielded the following results:

| Interstitial Elements | N | O | H | C |
|---|---|---|---|---|
| | 10 p.p.m. | 10 p.p.m. | 1 p.p.m. | 25 p.p.m. |

A resistivity ratio of the order of $10^3$, therefore, represents a very low impurity level.

### The dependence of flow stress on temperature and strain rate.

The applied shear stress which is required to cause plastic deformation is given by

$$\tau = \tau^* + \tau_A$$

where $\tau$ is the applied shear stress, $\tau^*$ is the stress required to aid the thermal activation of the rate controlling mechanism and therefore decreases precipitously as T increases. $\tau_A$ is the stress required to overcome any athermal barriers and it decreases only modestly as the temperature decreases, usually in parallel with the shear modulus of elasticity.

The primary interests of this work lie in the strain rate and temperature dependence of the thermal component of the stress. The results are presented in Fig. 3 and Fig. 4. The flow stresses decreased rapidly from 25°K to 425°K for both strain rates. Tests below 25°K were not performed due to the difficulties in controlling the stability of temperature. The curves (Figs. 3 and 4) were extrapolated to 0°K.

The thermal component of the stress, $\tau^*$, can be expressed as

$$\tau^* = \tau_T - \tau_{550°K} \frac{G\{T\}}{G\{550°\}}$$

where $\tau_T$ is the total resolved shear stress for flow at temperature T°K. $G\{T\}$ is the shear modulus of elasticity at temperature T°K. The term $\tau_{550°K} \frac{G\{T\}}{G\{550°\}}$ is the total back stress, corrected for the change in shear modulus with temperature. The variation of shear modulus with temperature was calculated from data obtained by Bolef and De Klerk[11] (Fig. 5).

The plastic strain rate, $\dot{\gamma}$, for a thermally activated process is given by

$$\dot{\gamma} = \rho abv\frac{L}{w} e^{-(U_n\{\tau^*\})}$$

where $\rho$ = density of mobile dislocations

    a = the distance between Peierls' valleys

    b = Burgers' vector

    L = the mean length swept out by a pair of kinks once nucleation occurs in that length

    w = width of a pair of kinks at the saddle point energy configuration

    $\nu$ = the Debye frequency

$U_n\{\tau^*\}$ = saddle point free energy for nucleation of pairs of kinks

    k = Boltzmann constant

    T = absolute temperature

When the testing temperature reaches a critical temperature, $T_c$ for a given strain rate, the thermal component of the stress, $\tau^*$, becomes zero and the activation energy at this condition is $2U_k$, where $U_k$ is the energy of a single kink. Therefore, at $T = T_c$

$$\dot{\gamma} = \rho ab\nu \, \frac{L}{w} \, e^{-\frac{2U_k\{T_c\}}{kT}}$$

The theory of Dorn and Rajnak predicts a universal relationship between $U_n/2U_k$ ($U_n$ is the saddle-point free energy for nucleation of a pair of kinks) and $\tau^*/\tau_p$, and the quantity $U_n/2U_k$ can be approximated by $T/T_c$. It is the purpose of this work to correlate the relationship predicted by the theory with that obtained from experimental results. It is shown in Figs. 6 and 7 that most of the experimental results at low temperatures (from 25°K to 425°K for $\dot{\gamma} = 9.9 \times 10^{-5}$ sec$^{-1}$, and from 77°K to 500°K for $\dot{\gamma} = 9.2 \times 10^{-3}$ sec$^{-1}$) fall on the theoretical

curve ($\alpha = 0$). At higher temperatures (from 425°K to 490°K for $\dot{\gamma}$ = 9.9 x $10^{-5}$ sec$^{-1}$, and from 500°K to 575°K for $\dot{\gamma}$ = 9.2 x $10^{-3}$ sec$^{-1}$), experimental results do not agree exactly with the theory (as shown in Fig. 7). A similar but more pronounced phenomenon was reported by Wynblatt et al.[9] in Iron-2% Mn alloys, but was not observed in tests on AgMg[7] and $Ag_2Al$.[8]

There are several possibilities to account for this disagreement with the theory. An obvious possibility is that the Peierls' hill has a slightly different shape from that assumed by Dorn and Rajnak. It is also possible that some other unknown mechanisms take over in this region. Another possibility is due to the slight weakness of the theory at the low stresses region. The theory neglects the reverse motion of the kink pair once passed over the Peierls' hill. Experimental errors might also be another explanation for this disagreement although great effort has been made to eliminate this possibility (the controllable variables were temperatures and strain rates).

Critical temperatures were obtained by plotting the high temperature results on the theoretical curves, and critical temperatures were read off from the scale (Appendix 2). The same method was applied to the low temperature results to calculate the Peierls' stress $\tau_p$. The calculated value of $\tau_p$ agreed very well with the extrapolated value from the experimental data. The agreement proves that this method of obtaining critical temperatures was a reasonably valid one. (The estimated error of the critical temperatures was about ±15°C.)

Experimental results are presented in Table I.

Table I

| T $^\circ$K | $\tau^* \times 10^{-8}$ dynes/cm$^2$ | |
| --- | --- | --- |
| | $\dot{\gamma} = 9.9 \times 10^{-5}$ sec$^{-1}$ | $\dot{\gamma} = 9.2 \times 10^{-3}$ sec$^{-1}$ |
| 25 | 36.40 ± .03 | |
| 52 | 31.07 | |
| 77 | 26.79 | 30.13 ± .03 |
| 153 | 19.33 | 22.49 |
| 196 | 15.70 | |
| 273 | | 13.87 |
| 296 | 8.68 | 12.65 |
| 425 | .61 | 3.49 |
| 450 | .41 | |
| 475 | .28 | |
| 500 | | 1.07 |
| 550 | 0 | .37 |
| 600 | 0 | 0 |

$\tau_p$ (extrapolated) = (41.9 ± 0.2) × 10$^8$ dynes/cm$^2$

$\tau_p$ (from theoretical curve) = (42.1 ± 0.2) × 10$^8$ dynes/cm$^2$

$Tc_1 = 442^\circ \pm 15^\circ$K

$Tc_2 = 513^\circ \pm 15^\circ$K

## Activation volume.

The quantity $\frac{\partial U_n}{\partial \tau^*}$ is defined as the activation volume which approximates the product of Burgers' vectors and the area swept our during the nucleation of the critical loop. The Peierls' mechanism has a unique

low value of the activation volume (usually ranging from 5 $b^3$ to 50 $b^3$[1]).
The activation volume also stays constant with increasing strain.
These properties of the activation volume are the most reliable verification
of the Peierls' mechanism. The properties of activation volume of
other suggested mechanisms are presented in Table II.

Table II

| Mechanism | Properties |
|---|---|
| Breaking away from an interstitial atmosphere | (1) Va depends on interstitial content. Very high values of Va.(probably up to 1000 $b^3$) |
| Nonconservative motion of jogs | (1) Va depends on structure. |
| | (2) Athermal at low temperature, thermally activated when $T > Tm/2$ |
| | (3) Va = $L_j b^2$.($L_j$ = length of jog) |
| Overcoming interstitial precipitates | (1) Va varies with impurity content. |
| | (2) Va = Li$b^2$. (Li = length of precipitate) |
| Cross slip | (1) High activation volume. (of the order of 700 $b^3$ - 800 $b^3$) |

The experimental activation volumes are obtained by the effect of
small changes in strain rate on the flow stress. A quantity $\beta$ is
defined as

$$\beta = \frac{\partial \ln \dot{\gamma}}{\partial \tau^*} = \frac{\partial \ln \rho}{\partial \tau^*} - \frac{\partial \ln w}{\partial \tau^*} - \frac{1}{kT}\frac{\partial U_n}{\partial \tau^*}$$

$\beta kT$ is defined as the apparent activation volume:

$$V_a = \beta kT = kt\,\frac{\partial \ln\rho}{\partial \tau^*} - kT\,\frac{\partial \ln w}{\partial \tau^*} - \frac{\partial U_n}{\partial \tau^*}$$

The negative of the last term is the theoretical activation volume. The term containing $w$ is always negligibly small. Therefore the apparent activation volume can be slightly larger than the theoretical one due to the increase in dislocation density, $\rho$, as the stress is increased. Figure 8 shows the apparent activation volume as a function of stress; the low values of $V_a$ are in good agreement with the low activation volume predicted by the Peierls' mechanism. Figure 9 also shows the relatively constant value of apparent volume with respect to strain. The theoretical and experimental values of activation volume are shown in Fig. 10, indicating the right order of magnitude of the experimental results.

## Activation energy of pairs of kinks.

The activation energy at $0°K$ can be measured by the change in strain rate due to the change of temperature.

$$\dot{\gamma} = \dot{\gamma}_o\, e^{-U_n/kT}$$

where

$$\dot{\gamma}_o = \rho ab\,\frac{L}{w}\,v$$

$$U_n = 2U_n - \tau^*\, v$$

at critical temperatures

$$\dot{\gamma}_1 = \dot{\gamma}_o\, e^{\frac{2U_k\{Tc_1\}}{kTc_1}}$$

$$\dot{\gamma}_2 = \dot{\gamma}_o \, e^{\dfrac{2U_k\{Tc_2\}}{kTc_2}}$$

Since $\dot{\gamma}_o$ stays constant for both cases,

$$\therefore \frac{\dot{\gamma}_2}{\dot{\gamma}_1} = \frac{\exp - [\dfrac{2U_k\{Tc_2\}}{kTc_2}]}{\exp - [\dfrac{2U_k\{Tc_1\}}{kTc_1}]} = \frac{\exp - [\dfrac{2U_k\{0\}}{kTc_2} \cdot \dfrac{G\{Tc_2\}}{G\{0\}}]}{\exp - [\dfrac{2U_k\{0\}}{kTc_1} \cdot \dfrac{G\{Tc_1\}}{G\{0\}}]}$$

or

$$2U_k\{0\} = \frac{kG\{0\}}{\dfrac{G\{Tc_1\}}{Tc_1} - \dfrac{G\{Tc_2\}}{Tc_2}} \quad \ln \frac{\dot{\gamma}_2}{\dot{\gamma}_1}$$

substituting

$$k = 1.38 \times 10^{-6} \text{ ergs/}^{\circ}K$$

$$G\{0\} = (1.372 \pm .001) \times 10^{12} \text{ dynes/cm}^2$$

$$G\{Tc_1\} = (1.297 \pm .001) \times 10^{12} \text{ dynes/cm}^2$$

$$Tc_1 = 442^{\circ}K \pm 15^{\circ}$$

$$Tc_2 = 513^{\circ}K \pm 15^{\circ}$$

$$\ln \frac{\dot{\gamma}_2}{\dot{\gamma}_1} = 4.52$$

$$\therefore \, 2U_k\{0\} = 2.0 \pm .4 \times 10^{-12} \text{ ergs} = 1.2 \pm .2 \text{ e.v.}$$

## Line tension of dislocation situated at the Peierls' valley.

As shown by Dorn and Mitchell[13]

$$\frac{2\pi U_k\{0\}}{a\Gamma_o} = 5.66 \left[\frac{\tau_p^* ab}{\pi \Gamma_o}\right]^{1/2}$$

where

$$a \simeq b = 2.73 \times 10^{-8} \text{ cm}$$

$$2U_k = 2.0 \pm .4 \times 10^{-12} \text{ ergs}$$

$$\tau^* \text{ (extrapolated)} = 41.9 \pm .2 \times 10^8 \text{ dynes/cm}^2$$

Solving for $\Gamma_o$; we have $\Gamma_o = 1.5 \pm .1 \times 10^{-3}$ dynes.

The line tension is also related to G and b by the equation

$$\Gamma_o = \delta G\{0\}b^2$$

$$\delta \simeq 1.5$$

This value compared with Nabarro's estimation of line tension $(\frac{Gb^2}{2})$ proves to be of the right order of magnitude.

<u>Experimental value of the number of dislocations per unit length ($\rho L$).</u>

For a given strain and temperature, the value of $\rho L$ can be determined from the equation

$$\dot{\gamma} = \rho ab \frac{L\nu}{w} e^{-(2U_k - \tau^*v)/kT}$$

The Debye frequency was calculated to be $9.38 \times 10^{12}$ per sec from the Debye characteristic temperature of molybdenum. Taking 60 b for the value of $w_c$ and substituting the values of a, b, $2U_k$, k and $T_c$, it was found that $\rho L$ was $3.5 \times 10^5$ per cm. This value seems to be somewhat high when compared with that of AgMg (227 per cm)[7] and Ta (104 per cm).[15] It is, nevertheless, a possible number in terms of the possibility of a high dislocation density.

An attempt was made to correlate the data with another model proposed by Dorn and Rajnak.[2] In this model, Dorn and Rajnak assumed

that several kinks may be moving along length L at one time, instead of only a single pair of kinks.  However, it was proven that this model cannot rationalize the present data.

## CONCLUSIONS

(1)  The strong temperature dependence of the flow stress below 425°K can be explained by the Dorn and Rajnak theory of the Peierls' mechanism of plastic deformation.

(2)  From 425°K to 600°K, the experimental results do not agree exactly with the theory, there is a possibility that the Peierls' hill has a slightly different shape than that assumed or that some unidentified mechanism takes over in this region.

(3)  The shape of the Peierls' hills for molybdenum seems to approach a purely sinusoidal variation with $\alpha = 0$ except perhaps near the bottom of the hill.

(4)  The calculated activation volume and line tension are in agreement with the theory.

## ACKNOWLEDGEMENT

## REFERENCES

1. H. Conrad, "Yielding and Flow of the B.C.C. Metals at Low Temperatures", Symposium on the Relation between Structure and Properties of Metals, National Physical Laboratory, Teddington, England (1962).

2. J. E. Dorn and S. Rajnak, Trans. AIME, 230, 1052 (1964).

3. J. W. Christian and B. S. Masters, Proc. Roy. Soc. A, 281, 240 (1964).

4. A. Seeger, Phil. Mag., 1, 651 (1956).

5. J. Lothe and J. P. Hirth, Phys. Rev., 115, 543 (1959).

6. H. Suzuki, J. Phys. Soc. Jap., 18, 182 (1963).

7. A. K. Mukherjee and J. E. Dorn, Trans. AIME, 230, 1065 (1964).

8. A. Rosen and J. E. Dorn, Trans. AIME, 230, 1065 (1964).

9. P. Wynblatt, A. Rosen and J. E. Dorn, Trans. AIME, 233, 652 (1965).

10. T. E. Tietz and J. W. Wilson, "Behavior and Properties of Refractory Metals", Stanford Univ. Press (1965).

11. D. I. Bolef and J. De Klerk, J. Appl. Phys., 33, No. 7, 2311-2314 (1962).

12. T. E. Mitchell and A. Spitzig, "Three-Stage Hardening in Tantalum Single Crystals", Case Inst. of Tech., sub. to Acta Met.

13. J. E. Dorn and J. B. Mitchell, "High Strength Materials", ed. by V. Zackay, John Wiley and Sons, Inc., 510-577 (1965).

14. L. Van Torne and G. Thomas, to be published in J. Less Com. Metals.

15. S. Ranji, private communication.

## FIGURE CAPTIONS

1. Schematic diagram showing the nucleation of a pair of kinks.

2. Orientation of tensile axis of the specimen.

3. 0.2% flow stress, $\tau$, vs. temperature.

4. The thermally activated 0.2% flow stress, $\tau^*$, vs. temperature.

5. Variation of shear modulus G in [111] ($\bar{1}$01) system with temperature.

6. The thermally activated flow stress vs. temperature in dimensionless units.

7. The thermally activated flow stress vs. temperature (theoretical curve, $\alpha = 0$, included).

8. Apparent activation energy vs. thermally activated flow stress.

9. Apparent activation volume at 373°K vs. strain.

10. The thermally activated component of flow stress vs. activation volume in dimensionless units.
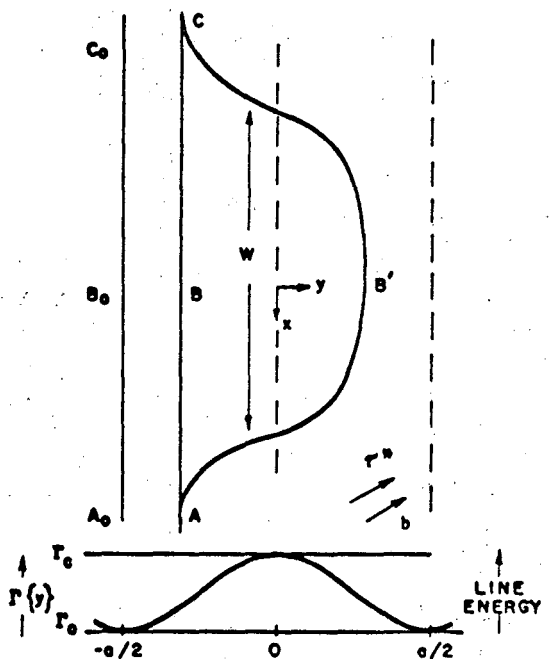
FIG. 1.   NUCLEATION OF A PAIR OF KINKS.
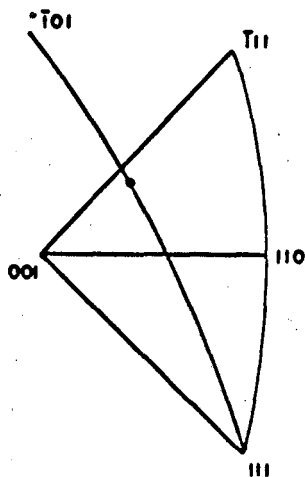


FIG. 2.   ORIENTATION OF TENSILE AXIS
OF THE SPECIMEN.

MU-37181
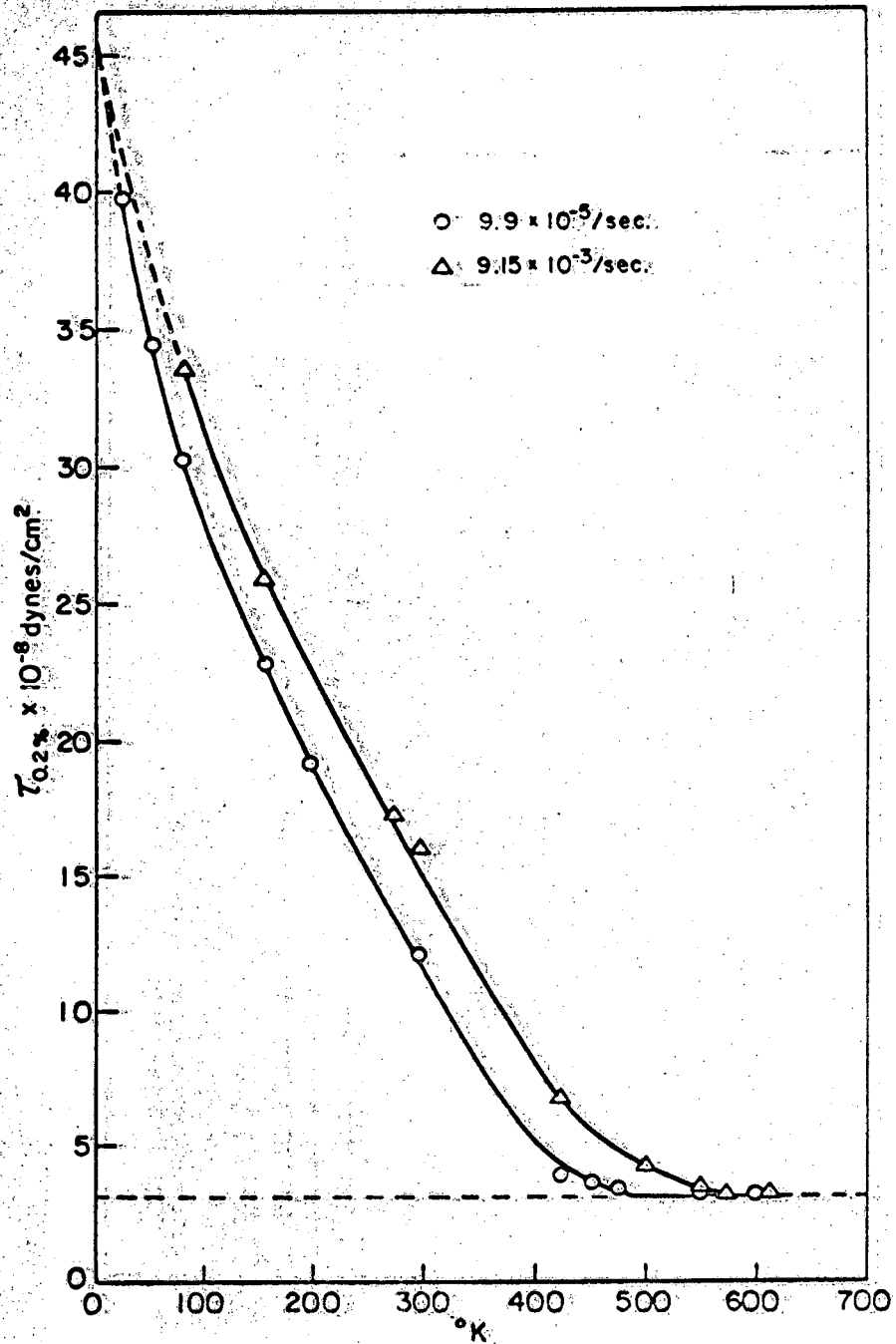
FIG. 3. 0.2% FLOW STRESS vs. TEMPERATURE.
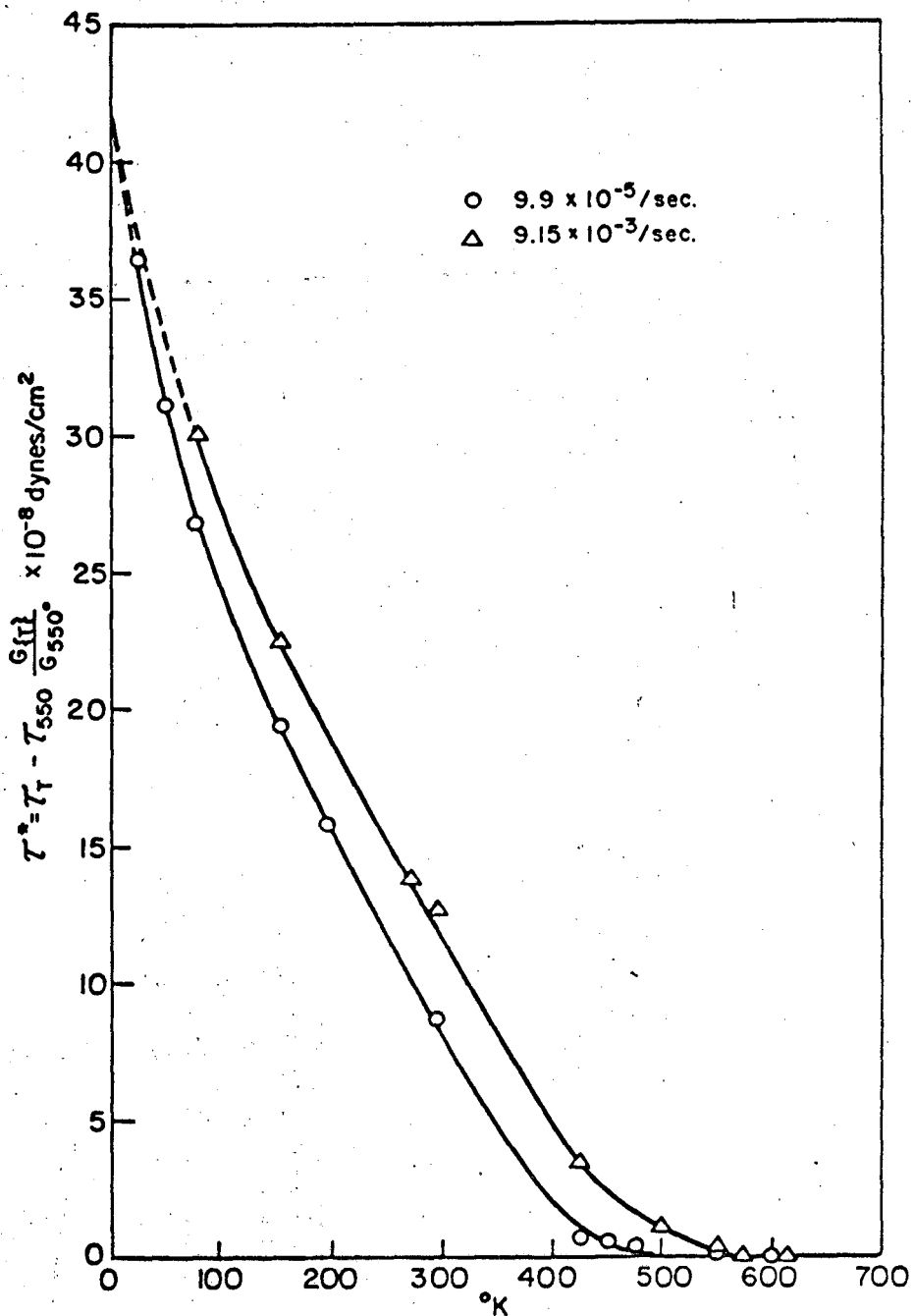
M.U.-37182

FIG. 4. THERMALLY ACTIVATED 0.2% FLOW STRESS vs. TEMPERATURE.
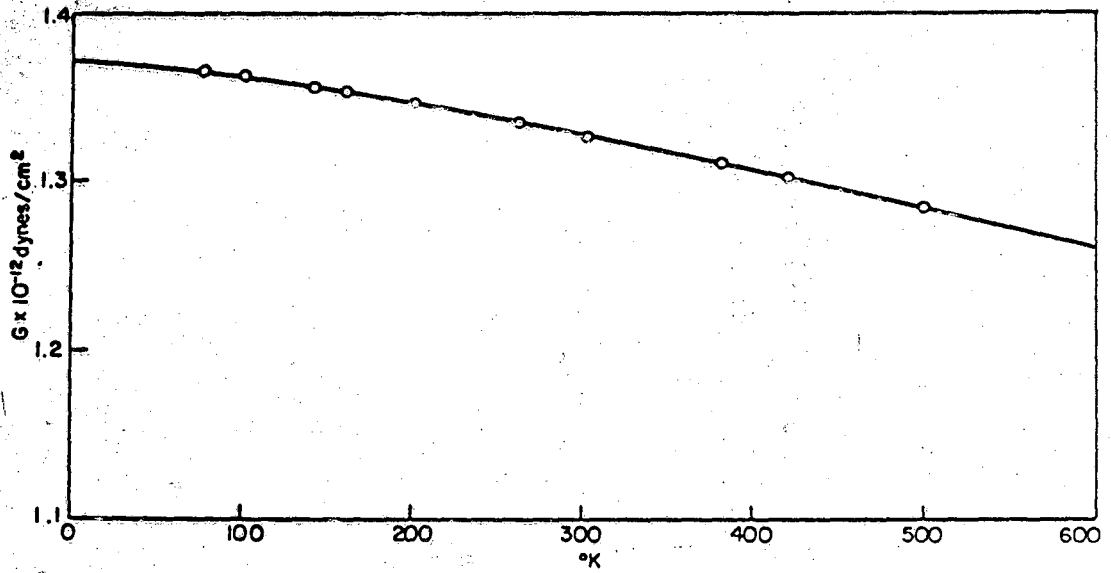
MU-37183

FIG. 5 VARIATION OF SHEAR MODULUS G IN (̄I01) [III] SYSTEM WITH TEMPERATURE.

MU-37184
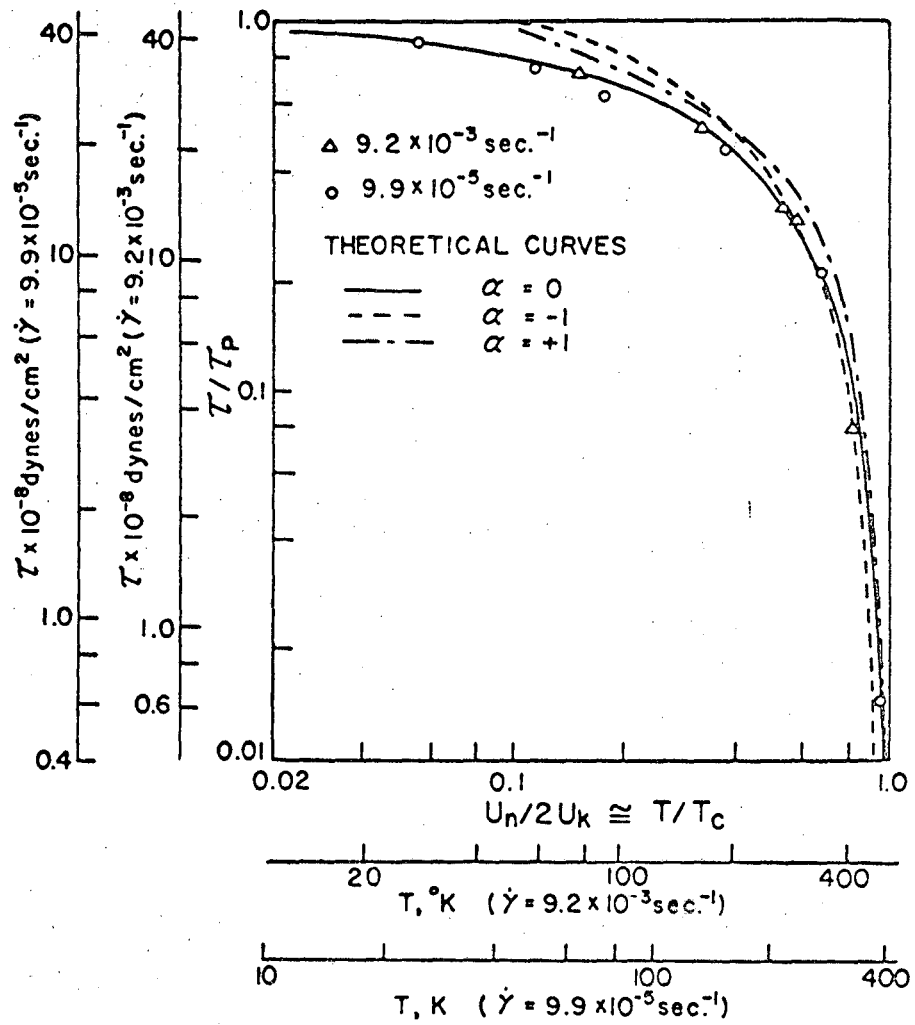
FIG. 6. THERMALLY ACTIVATED FLOW STRESS vs. TEMPERATURE IN DIMENSIONLESS TIME.

MU.37185
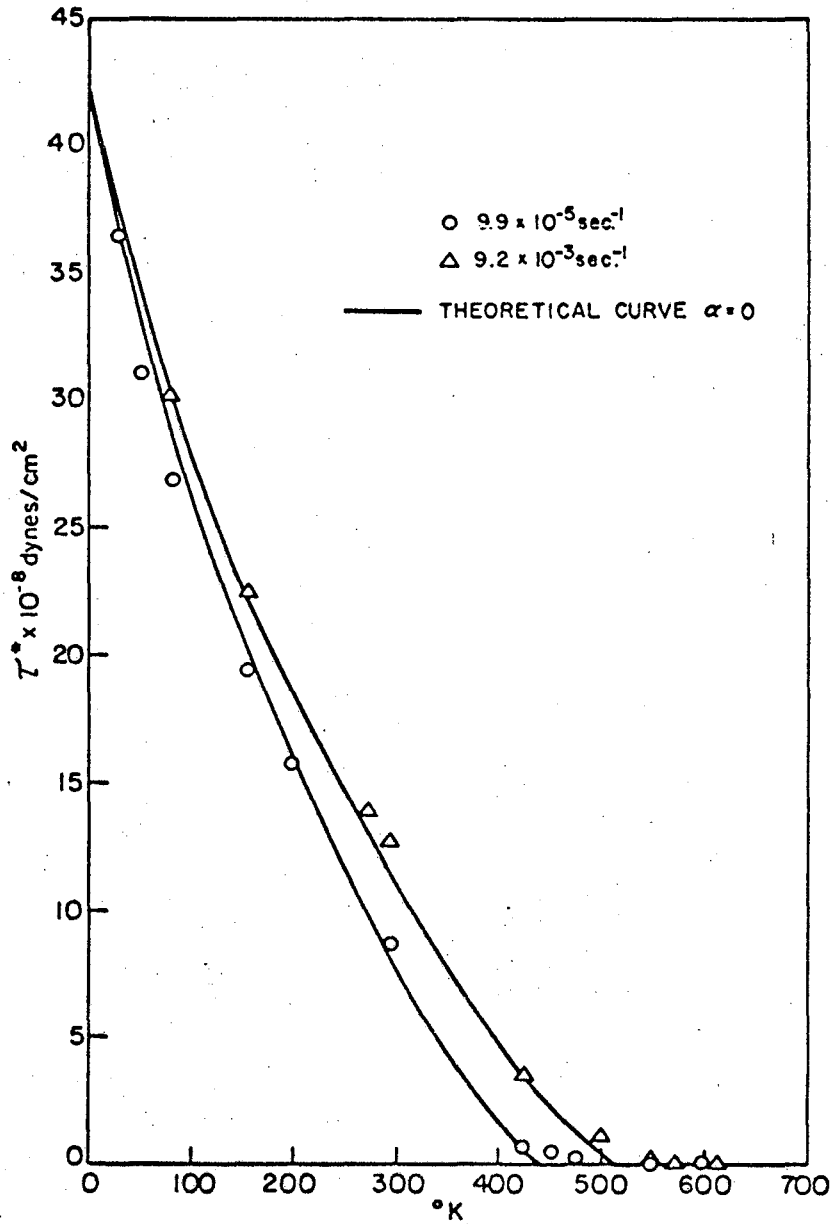
FIG. 7. THERMALLY ACTIVATED 0.2% FLOW STRESS vs. TEMPERATURE SHOWING THEORETICAL CURVES.

MU.37186
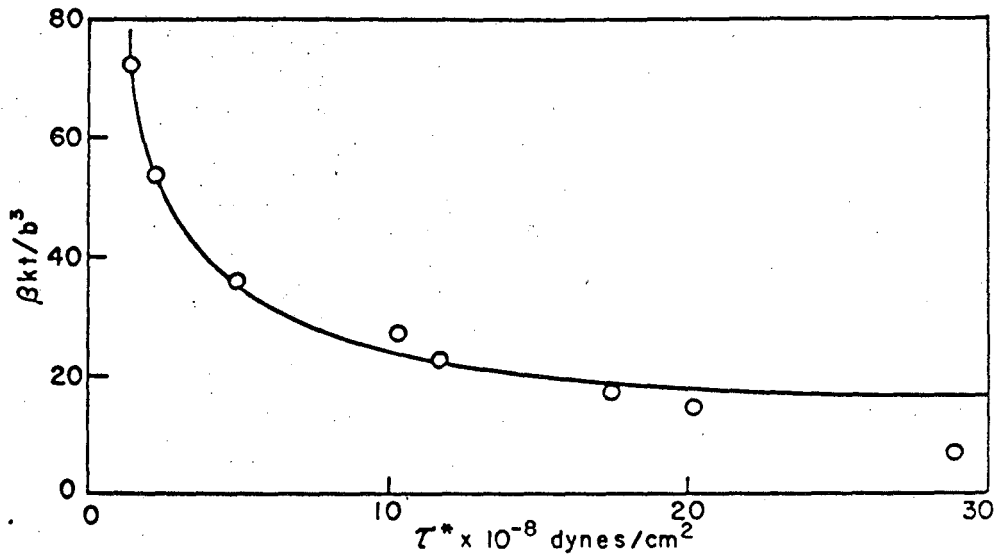
FIG. 8. APPARENT ACTIVATION ENERGY vs. THERMALLY
ACTIVATED 0.2 % FLOW STRESS.
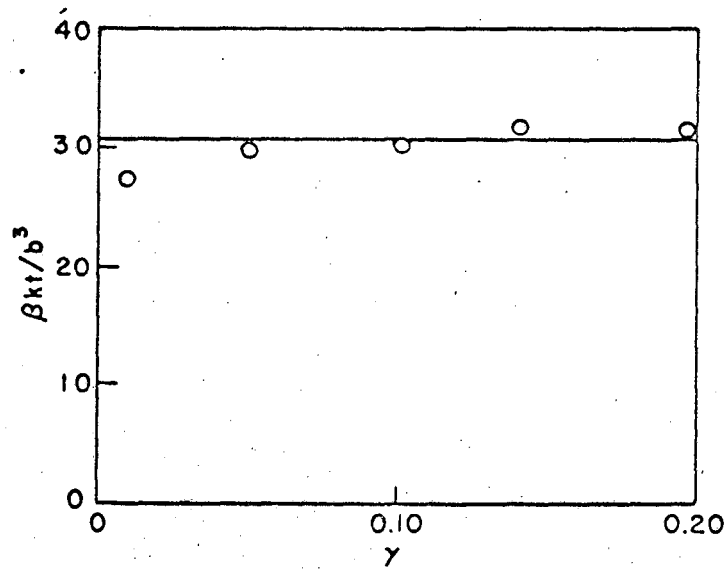


FIG. 9. APPARENT ACTIVATION VOLUME AT
373 °K vs. STRAIN.
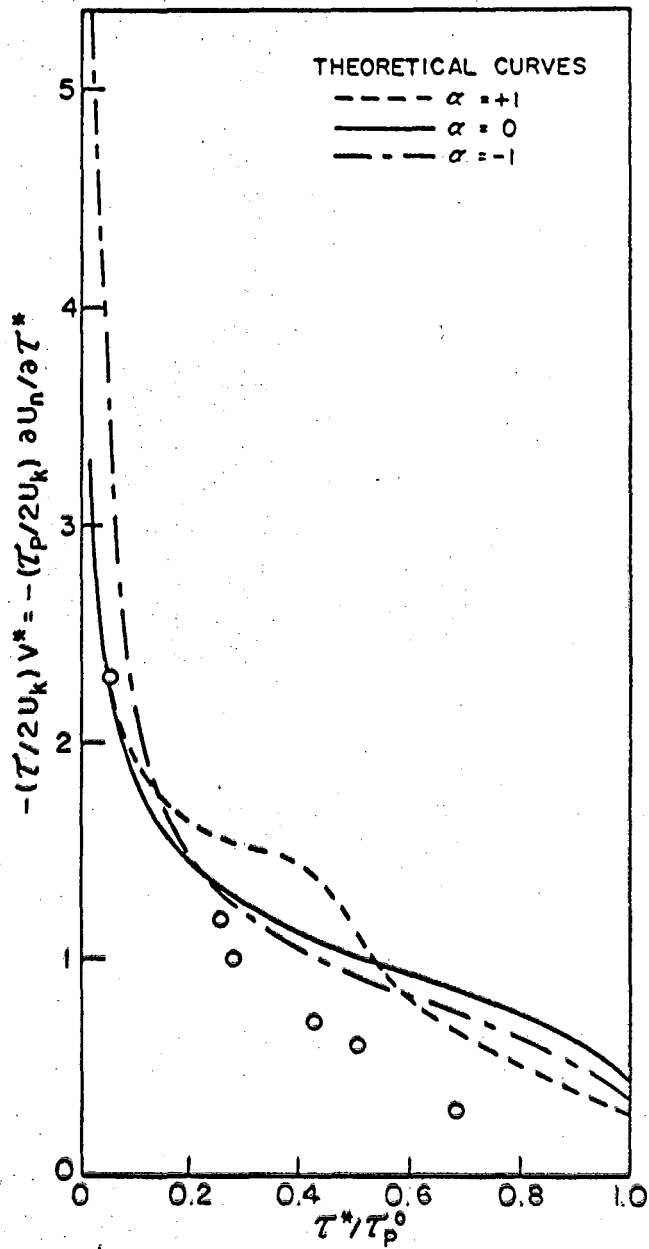
MU-37187

FIG. 10 THE THERMALLY ACTIVATED
COMPONENT OF FLOW STRESS vs.
ACTIVATION VOLUME IN DIMENSIONLESS TIME.

MU.37188

## APPENDIX 1

Resolved shear strains and stresses of a single slip system:

$$\gamma = \frac{\sqrt{(\ell/\ell_o)^2 - \sin^2 \lambda_o} - \cos \lambda_o}{\sin x_o}$$

$$\tau = \frac{L}{A_o} \sin x_o \sqrt{1 - \left(\frac{\ell_o}{\ell}\right)^2 (\sin \lambda_o)^2}$$

$\ell_o$ = original gauge length

L = load

$A_o$ = original cross section area

## APPENDIX 2

Determination of critical temperatures from Fig. 6:

For the theoretical curve $\alpha = 0$

$$\dot{\gamma} = 9.2 \times 10^{-3} \text{ sec}^{-1}$$

The experimental point
$$\begin{cases} T = 425°K \\ \tau^* = 3.49 \times 10^8 \text{ dynes/cm}^2 \end{cases}$$

coincides with the point
$$\begin{cases} T/T_c = .83 \\ \tau^*/\tau_p = .079 \end{cases}$$
on the theoretical curve $\alpha = 0$

(as shown in Fig. 6), therefore, solving for $Tc_2$, $Tc_2 = \frac{425}{.83} = 513°K$.

For $\dot{\gamma} = 9.9 \times 10^{-5} \text{ sec}^{-1}$

The experimental point
$$\begin{cases} T = 425°K \\ \tau^* = .61 \end{cases}$$

coincides with the point
$$\begin{cases} T/T_c = .96 \\ \tau/\tau_p = .0144 \end{cases}$$
on the theoretical curve $\alpha = 0$ (as shown in Fig. 6)

solving for $Tc_1$, $Tc_1 = \frac{425}{.96} = 442°K$.

The same method applied to $\tau_p^o$ for low temperature experimental points, one gets the following results:

$$\alpha = 0$$

$$\dot{\gamma} = 9.9 \times 10^{-5} \text{ sec}^{-1}$$

$$\begin{cases} T = 25°K \\ \tau = 36.4 \times 10 \quad \text{dynes/cm}^2 \end{cases}$$

coincides with $\begin{cases} T/T_c = .56 \\ \tau/\tau_p = .86 \end{cases}$

therefore $\tau_p = 42.4 \times 10^8$ dynes/cm$^2$

$$\dot{\gamma} = 9.2 \times 10^{-3} \text{ sec}^{-1}$$

$$\begin{cases} \tau = 30.13 \times 10^8 \text{ dynes/cm}^2 \\ T = 77.K \end{cases}$$ coincides with $\begin{cases} T/T_c = .15 \\ \tau/\tau_p = .72 \end{cases}$

therefore $\tau_p = 41.8 \times 10^8$ dynes/cm$^2$.

The average value $\bar{\tau}_p = 42.1 \times 10^8$ dynes/cm$^2$ as compared to $\tau_p$ (extrapolated) $= 41.9 \times 10^8$ dynes/cm$^2$ proves that the extrapolation is a satisfactory one.

## APPENDIX 3

Relation between shear modulus and shear constants of $[111]$ $[\bar{1}01]$ slip system.

$$\frac{1}{G_{[111](\bar{1}01)}} = S_{44} + 4(S_{11} - S_{12} - \frac{S_{44}}{2})\,H$$

where $H$ = geometric factor = 1/3 for $[111][\bar{1}01]$ slip system.

Therefore:

$$\frac{1}{G_{[111](\bar{1}01)}} = \frac{1}{C_{44}} + \frac{4}{3}\left(\frac{1}{C_{11}-C_{12}} - \frac{1}{2C_{44}}\right)$$